TRANSFER MATRIX MODELLING OF HYDRAULICALLY ACTUATED FLEXIBLE ROBOTS

Ryan Krauss[1], Wayne Book[2], and Olivier Brüls[3]

[1]*Southern Illinois University Edwardsville*
[2]*Georgia Institute of Technology*
[3]*University of Liège, FNRS*

Abstract

Accurate models of hydraulic motors and their interaction with flexible structures are needed to design motion control and vibration suppression schemes for hydraulically actuated flexible robots. The modeller of such a system faces significant challenges including capturing the dynamics of the actuator, integrating the actuator model into the system model, incorporating distributed parameter elements into the system model, determining any unknown model parameters, and creating a model that is useful for control design. This paper presents a model that overcomes all of these challenges. A transfer matrix model of a hydraulic actuator interacting with a flexible robot is developed. This model is integrated into a system model for a flexible robot. The model captures the interaction between the actuator and the structure and has been experimentally validated.

Keywords: transfer matrix method, flexible robots, modelling, vibration suppression, control design

1 Introduction

Flexible robots can be lighter, faster, and cheaper to actuate than rigid robots. In order to realize these benefits, some means of dealing with the associated vibration problems is required. If a flexible robot is hydraulically actuated, accurate models of the interaction between the actuator and the structure are needed so that motion control and vibration suppression systems can be designed.

From the standpoint of a control engineer, it would be ideal if these models accurately captured the essential dynamics without being unnecessarily complicated.

This paper presents a model of hydraulic actuators interacting with flexible robots or structures. This model is based on the transfer matrix method (TMM) (Pestel and Leckie, 1963). The TMM is well-suited for modelling and control design of flexible robots because it is modular, it handles serial connections of components extremely well, it naturally outputs Bode plots, and it can model distributed parameter elements such as flexible robot links without discretization. The TMM model of a hydraulic actuator developed in this work allows the system dynamics to exert a disturbance torque on the rotary hydraulic motor and the actuator model integrates seamlessly with the model of the entire system. The model is experimentally validated.

Hydraulic actuators have some advantages over servo-motors or other electromagnetic actuators in certain applications, but they also bring some additional modelling challenges. Fluid power is able to deliver high forces at low speeds without further speed reduction (gearboxes) and thus is well suited to certain robotic applications. Hydraulic fluid can be used to carry away dissipated heat and hence allow higher power in confined spaces. Some of the modelling challenges include the fact that fluid power is not well approximated as a force source as is the case for electromagnetics. It is more like a velocity source in some cases, but its internal dynamics include compressibility that interacts with flexibility of the structure. Since this interaction becomes critical at system resonances, a realistic model of both structural flexibility and hydraulics is required for the purpose of motion and vibration control.

2 System Description

This paper focuses on modelling a hydraulically-actuated, flexible robot known as SAMII (Small, Articulated Manipulator II). A picture and schematic of SAMII are shown in Fig. 1. SAMII has 6 rigid links that are hydraulically actuated. SAMII is mounted on the end of a 5 meter long cantilever beam. This paper will specifically discuss modelling joint 2 of SAMII and the interaction between that joint and the structure.

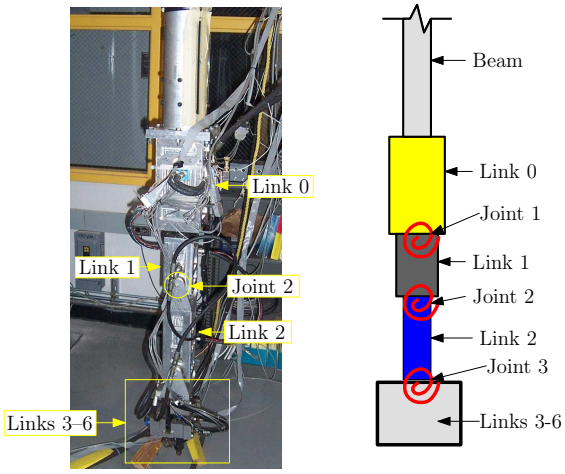

Fig. 1 *Picture and schematic of SAMII. Joint 2 is the actuated joint for the experimental Bode plots in this work.*

All of SAMII's joints are actuated by rotary hydraulic motors controlled by servo-valves. A schematic of an actuator is shown in Fig. 2. The double vane motor actuator used has a volumetric displacement of 0.01475 L/rad. The radius of the vane is 25.3 mm and the width of the vane is 11.7 mm. The valve supply pressure is 103 bar. The servovalve is a Moog Series 30. Modelling the amplifier, servo-valve, and motor together, the input is a voltage v that is proportional to spool position d. The output is angle of rotation θ.

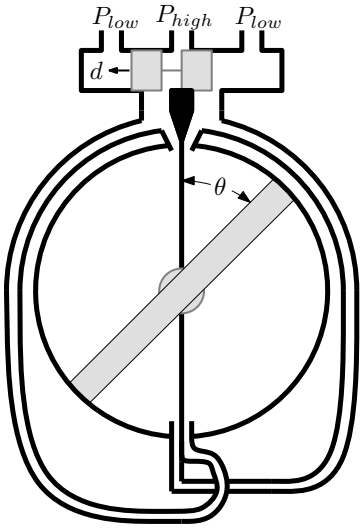

Fig. 2: *One of SAMII's hydraulic actuators, a rotary hydraulic motor controlled by a servo-valve*

3 Problem Statement

A simple transfer function model for a hydraulic actuator fails to capture the actuator/structure interaction near resonance. Consider a model that is an angular velocity source (AVS) with a first-order term:

$$\frac{\theta}{v} = \frac{K p}{s(s+p)} \qquad (1)$$

where v is the voltage into the amplifier, K is the actuator gain, p is the pole of the first-order term, and θ is the angular position of the joint.

Figure 3 compares Bode plots from this model and experimental data. While this model is fairly accurate for much of the frequency range, it breaks down near the second natural frequency of the structure at approximately 8 Hz.

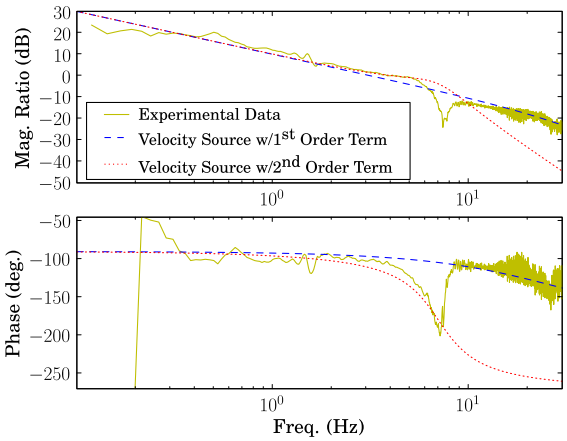

Fig. 3: *Comparison of actuator Bode plots θ/v from experimental data and from a models where the actuator is an angular velocity source with a first or second order term.*

Figure 3 also shows that a velocity source with a second-order term of the form

$$\frac{\theta}{v} = \frac{K\omega^2}{s(s^2 + 2\zeta w s + w^2)} \qquad (2)$$

also fails to accurately capture the dynamics of the system.

4 An Actuator Model Emulating Intrinsic Velocity Feedback

One potential explanation for the discrepancy between model and experiment in Fig. 3 is that the velocity source model assumes that the actuator can supply any magnitude of torque required. In an attempt to better capture the dynamics of the actuator, a model emulating intrinsic velocity feedback has been proposed (Obergfell, 1998; Krauss et al, 2005):

$$M = g_v(g_a v - \dot{\theta}) \qquad (3)$$

where M is the torque applied by the actuator, v is the voltage to the actuator, $\dot{\theta}$ is the angular velocity of the joint, and g_v and g_a are constants. A block diagram of this model is shown in Fig. 4.

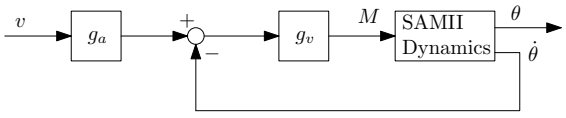

Fig. 4: *Block diagram of a hydraulic actuator model that emulates intrinsic velocity feedback.*

If $g_v \to \infty$, this model is equivalent to a velocity source model. For finite g_v, the transfer function between v and θ is affected by the system dynamics near resonances.

Figure 5 shows the results of using eq. (3) in a finite element analysis model of the system. This model shows some improvement over the velocity source model of Fig. 3: there is interaction between the actuator and structure at resonances. However, there is still significant error in the phase of the model. The model predicts a phase dip at the second natural frequency of 20–30° followed by an increase in phase above the nominal value before resonance of the same magnitude. The experimental results show a phase dip of about 90° at the second natural frequency, followed by a phase recovery but no increase.

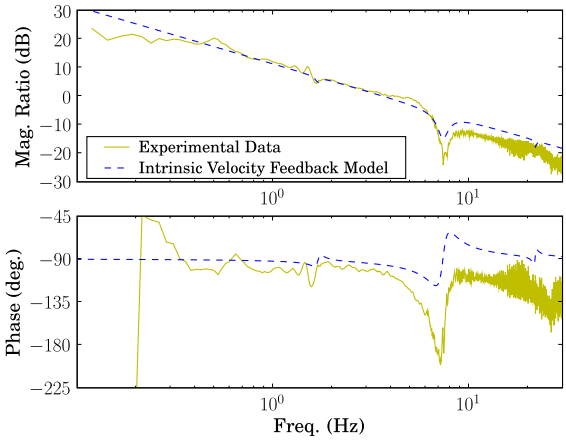

Fig. 5: *Comparison of actuator Bode plots θ / v from experimental data and from an intrinsic velocity feedback model.*

Attempting to better model the actuator torque dynamics seems to show promise, but the model of eq. (3) does not seem to be the final answer. An experimental investigation was undertaken to better understand the torque dynamics of the actuator.

5 Torque Experiments

Figure 1 shows SAMII in the configuration used in the previous sections with all of links 0–6 attached. Fig. 6 shows the setup for the torque experiment testing. SAMII's links 2–6 have been removed and replaced with one, small, rigid link. There is a force/torque sensor installed between this rigid link and the output shaft of joint 2. Note that SAMII's base was rigidly connected to the floor for this testing, so that the flexibility of the supporting beam no longer influences the dynamics of the system. The torque testing was done in a vertical and a horizontal configuration. Figure 7 shows the difference between these two.

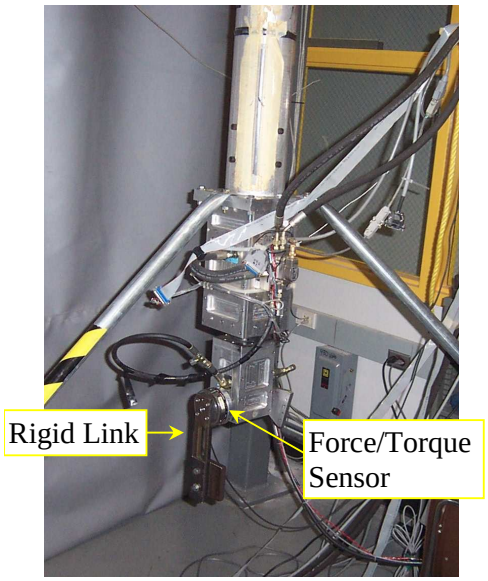

Fig. 6: *Set-up for testing in a vertical configuration.*

In the vertical configuration, gravity contributes a small torque, but one that is proportional to θ and is a restoring torque. As a result, the Bode plot for the vertical configuration in Fig. 8 is that of a pendulum with a torque input and angular position as the output. In the horizontal configuration, the gravity torque is larger, but nearly constant.

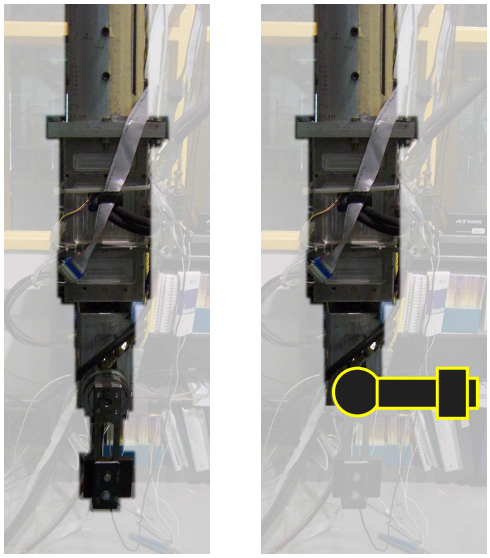

Fig. 7: *Set-up for torque experiments with the rigid link in vertical and horizontal configurations.*

Figure 8 shows the Bode plots for θ / M for the horizontal and vertical configurations. These Bode plots show the relationship between torque generated by the actuator and the resulting angular displacement. There is not an obvious input/output relationship between these two variables across the two different configurations.

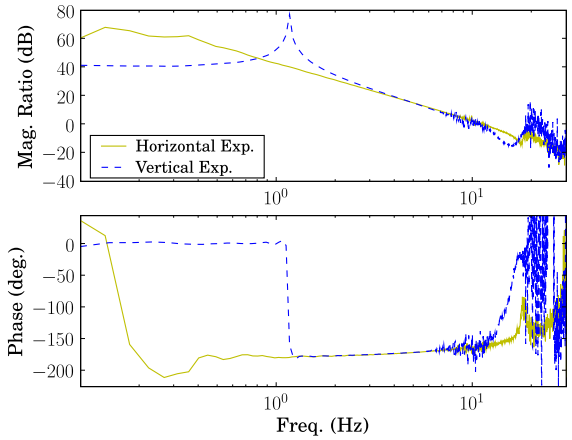

Fig. 8: *Bode plot of θ/M for the hydraulic actuator in horizontal and vertical configurations.*

Figure 9 shows the Bode plot for torque M vs. input voltage to the actuator v. For the vertical configuration, the sum of moments about the joint gives

$$J\ddot{\theta} + mgr\theta = M \qquad (4)$$

where m is the mass of the rigid link, g is the acceleration due to gravity, r is the distance from the joint to the center of gravity of the link, and J is the second moment of inertia of the link.

At low frequencies, the gravity part of this equation is dominant. This leads to torque that is proportional to θ. Assuming that v is roughly proportional to $\dot{\theta}$, $M/v \approx \theta/\dot{\theta} = 1/s$. At high frequencies, the inertia torque dominates and M is proportional to $\ddot{\theta}$. This leads to $M/v \approx \ddot{\theta}/\dot{\theta} = s$. These approximate low and high frequency relationships are seen in Fig. 9 and models based on eqs. (1) and (4) agree closely with experiments for both the vertical and horizontal positions.

In the horizontal configuration, the linearized sum of the moments is

$$J\ddot{\theta} + mgr = M \qquad (5)$$

so that M is proportional to $\ddot{\theta}$ and has a DC offset.

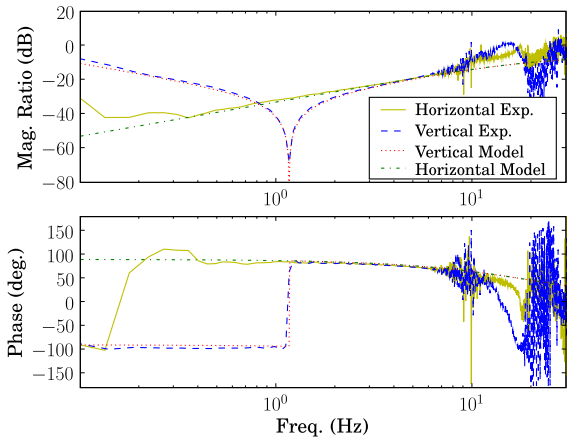

Fig. 9: *Bode plot of M/v for the hydraulic actuator in horizontal and vertical configurations.*

Figure 10 shows the Bode plots for angular position θ vs. input voltage to the actuator v. In both the horizontal and vertical configurations, the actuator acts as an integrator or a velocity source with $\dot{\theta}$ proportional to v.

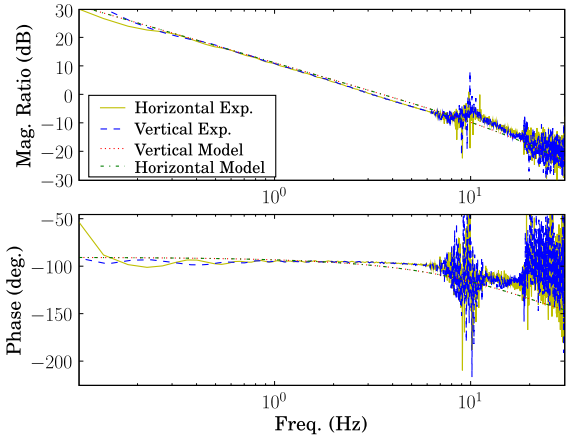

Fig. 10: *Bode plot of θ/v for the hydraulic actuator in horizontal and vertical configurations.*

Looking at the Bode plots of Figs. 8–10, the clearest input/output relationship is that of Fig. 10 where the relationship between θ and v is that of eq. 1. This relationship is the same in the vertical and horizontal configurations, so that gravity does not need to be explicitly considered in the model.

Equation (1) is an adequate model when the base of SAMII is rigidly connected to the floor, but it seems that in order to explain the interaction between the actuator and the deformation of the supporting beam at resonance, some local compliance needs to be added to the actuator model. The velocity source model should be combined with some means of incorporating the moment applied to the actuator from the structural dynamics as a disturbance input. To that end, the next section shows the results of combining an angular velocity source with a torsional spring/damper.

6 Transfer Matrix Modelling

The transfer matrix method (TMM) was used to model the actuator and its interaction with the structure. As mentioned in the introduction, there are several key advantages to using the TMM for modelling and control design of flexible robots. The TMM model of the hydraulic actuator easily incorporates the moment from the structural dynamics as a disturbance input (this will be discussed in section 6.1). Distributed parameter elements can be modelled without discretization, eliminating concerns about appropriate discretization of SAMII's cantilever beam. Integrating the actuator model into the overall system model is seamless. The TMM outputs Bode plots naturally and lends itself to control design. As part of this work, software has been developed that automates control design and system identification using TMM models.

The transfer matrix method was introduced by Pestel and Leckie (1963). It is a modelling approach

based on breaking a system into elements that are represented by matrices that transfer a vector of states from one end of the element to the other. A serially connected system is modelled by multiplying element transfer matrices together to form a system transfer matrix.

The TMM was applied to the design of flexible robots by Book (1974) and to the analysis of the remote manipulator system of the space shuttle by Book et al (1979, 1981). Book and Majette (1983) developed a means for using the TMM in state-space control design.

The underlying mathematical basis for the TMM is very similar to that of the dynamic stiffness method (DSM) (Hallauer and Liu, 1982; Banerjee, 1997). The DSM has been applied to a variety of structural dynamics problems by Banerjee and Fisher (1992) and others.

6.1 Angular Velocity Source in Series with a Torsional Spring/Damper

As an illustrative example of the use of the TMM, consider modelling the hydraulic actuator as an angular velocity source in series with a torsional spring/damper. The transfer function would be

$$\theta = \frac{K\,p\,v}{s(s+p)} + \frac{M}{cs+k} \tag{6}$$

where v is the command voltage, M is the moment from the dynamics of the structure, k and c are the spring and damping coefficients used to model compliance in the actuator, K is the actuator gain, and p is the pole of the first order lag. Note that this is significantly different from the model of eq. (2): there are two inputs, v and M, and M is essentially a disturbance input to the actuator that is coming from the dynamics of the system.

This model could be put in transfer matrix form:

$$\mathbf{U}_{ol} = \begin{bmatrix} 1 & 0 & 0 & 0 & 0 \\ 0 & 1 & \dfrac{1}{cs+k} & 0 & \dfrac{K\,pv}{s(s+p)} \\ 0 & 0 & 1 & 0 & 0 \\ 0 & 0 & 0 & 1 & 0 \\ 0 & 0 & 0 & 0 & 1 \end{bmatrix} \tag{7}$$

where $\mathbf{U}_{ol}$ refers to the open-loop actuator transfer matrix. The state vector would be

$$\mathbf{z} = \begin{Bmatrix} w \\ \theta \\ M \\ V \\ 1 \end{Bmatrix} \tag{8}$$

where w is the lateral displacement, θ is the rotation, M is the moment, and V is the shear force. The states before and after the actuator would be related by

$$\mathbf{z}_{after} = \mathbf{U}_{ol}\,\mathbf{z}_{before} \tag{9}$$

The second row of eq. (9) gives

$$\theta_{after} = \theta_{before} + \frac{M}{cs+k} + \frac{K\,pv}{s(s+p)} \tag{10}$$

Defining the relative angle across the actuator as

$$\theta = \theta_{after} - \theta_{before} \tag{11}$$

shows that the TMM model of eq. (9) is identical to the transfer function model of eq. (6).

6.2 TMM System Model

A schematic of SAMII with links 0–6 attached is shown in Fig. 11. The corresponding system transfer matrix would be

$$\mathbf{U}_{sys} = \mathbf{U}_{base}\,\mathbf{U}_{beam}\,\mathbf{U}_{l0}\,\mathbf{U}_{j1}\,\mathbf{U}_{l1}\,\mathbf{U}_{ol}\,\mathbf{U}_{l2}\,\mathbf{U}_{j3}\,\mathbf{U}_{l3-6} \tag{12}$$

where $\mathbf{U}_{l0}$, $\mathbf{U}_{l1}$, $\mathbf{U}_{l2}$, and $\mathbf{U}_{l3-6}$ are rigid body transfer matrices modelling links 0, 1, 2, and 3–6 respectively. $\mathbf{U}_{j1}$ and $\mathbf{U}_{j3}$ are torsional spring/damper transfer matrices modelling unactuated joints 1 and 3. $\mathbf{U}_{base}$ is a torsional spring/damper transfer matrix representing flexibility in the clamp at the top of the cantilever beam. $\mathbf{U}_{beam}$ is the transfer matrix for a continuous beam element.

Figure 12 compares Bode plots from this TMM model with experimental data and the intrinsic velocity feedback model discussed in section 4. The values for c, k, and p from the model of eq. (10) were found using an optimization algorithm that seeks to minimize the squared sum of the error between model and experiment in Fig. 12. The TMM model that represents the actuator as an angular velocity source in series with a torsional spring/damper leads to better agreement with experiment than the intrinsic velocity feedback model. The interaction between the actuator and structure around 8 Hz is accurately modelled.

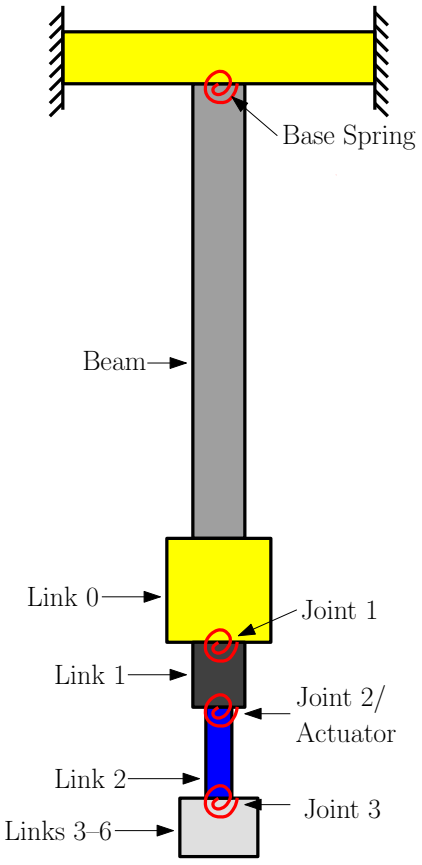

Fig. 11: *Schematic of SAMII with links 0–6 attached.*

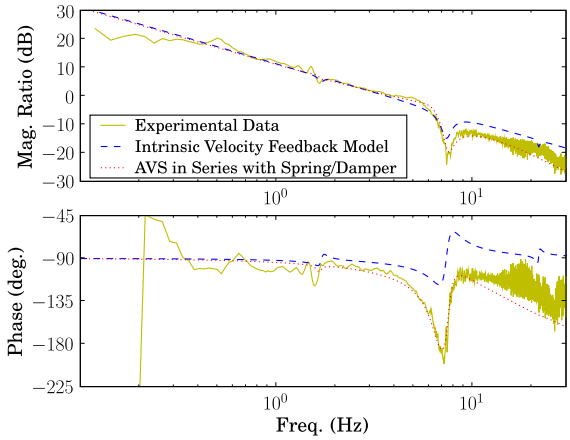

Fig. 12: *Overlay of Bode plots from experiment, an intrinsic velocity feedback model, and an angular velocity source (AVS) in series with a spring/damper.*

7 Conclusions

A transfer matrix model has been developed for a rotary hydraulic motor controlled by a servo-valve. This model accurately captures the interaction between the actuator and a flexible robot. The model includes a disturbance moment input to the actuator coming from the structural dynamics. The TMM formulation overcomes several challenges that modellers of flexible robots must face: the actuator model is seamlessly integrated into an overall system model, beam elements are modelled without discretization, and the model facilitates control design and system identification.

The model has been experimentally validated. One advantage of the approach is how cleanly actuator flexibility can be incorporated into the system model. The TMM formulation could also be used to model the actuator as its own distributed parameter system, possibly incorporating flexibility and linear damping in the hydraulic lines or compressibility in the fluid.

8 Acknowledgments

This work was supported by the Fluid Power and Motion Control Center at Georgia Institute of Technology. Olivier Brüls is supported by the Belgian National Fund for Scientific Research (FNRS) which is gratefully acknowledged.

Nomenclature

c	damping coefficient	[N m s/rad.]
g	acceleration due to gravity	[m/s^2]
g_a	voltage gain	[rad./(s V)]
g_v	velocity feedback gain	N m s/rad.
J	second moment of inertia	[kg m^2]
K	gain of actuator transfer function	[rad.^{2}/(s V)]
m	mass of rigid link	[kg]
M	torque	[N m]
p	pole of first order lag term	[rad./s]
r	distance between center of gravity and joint of rigid link	[m]
θ	angular position/displacement	[rad.]
$\dot{\theta}$	angular velocity	[rad./s]
$\ddot{\theta}$	angular acceleration	[rad./s^2]
v	input voltage to actuator	[V]
$\mathbf{U}$	transfer matrix	
$\boldsymbol{z}$	state vector	

References

Pestel, E. C. and **Leckie, F. A.** 1963. *Matrix Methods in Elastomechanics*. McGraw Hill, New York.

Obergfell, K. 1998. *End-Point Position Sensing and Control of Flexible Multi-Link Manipulators*. PhD thesis, Georgia Institute of Technology, School of Mechanical Engineering.

Krauss, R. W., Brüls, O., and **Book, W. J.** 2005. Two competing linear models for flexible robots: Comparison, experimental validation, and refinement. *Proceedings of the 2005 American Control Conference*.

Book, W. J. 1974. *Modeling, Design and Control of Flexible Manipulator Arms*. PhD thesis, Massachusetts Institute of Technology.

Book, W. J., Majette, M. W., and **Ma, K.** 1979. Distributed systems analysis package (dsap) and its application to modeling flexible manipulators. Final Report, NASA Subcontract No. 551 to Charles Stark Draper Laboratory, NASA Contract NAS9-13809.

Book, W. J., Majette, M. W., and **Ma, K.** 1981. Frequency domain analysis of the space shuttle manipulator arm and its payloads. Final Report, NASA Subcontract No. 586 to Charles Stark Draper Laboratory, NASA Contract NAS9-13809.

Book, W. J. and **Majette, M. W.** 1983. Controller design for flexible, distributed parameter mechanical arms via combined state space and frequency domain techniques. *Journal of Dynamic Systems, Measurement and Control, Transactions ASME*, Vol. 105(4), pp. 245–254.

Hallauer, W. L. and **Liu R. Y. L.** 1982. Beam bending-torsion dynamic stiffness method for calculation of exact vibration modes. *Journal of Sound and Vibration*, Vol. 85, pp. 105–113.

Banerjee, J. R. 1997. Dynamic stiffness formulation for structural elements: a general approach. *Computers & Structures(UK)*, Vol. 63(1), pp. 101–103.

Banerjee, J. R. and **Fisher, S. A.** 1992. Coupled bending-torsional dynamic stiffness matrix for axially loaded beam elements. *International Journal for Numerical Methods in Engineering*, 3 Vol. 3, pp. 739–751.

Ryan Krauss
Ryan Krauss is an assistant professor in the Mechanical Engineering Department at Southern Illinois University Edwardsville. He holds degrees from Georgia Tech (Ph.D.), Virginia Tech (M.S.), and Michigan Tech (B.S.). His research interests include modeling and control design of flexible systems, control implementation, and mechatronics.

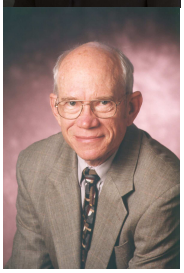

Wayne J. Book
Wayne J. Book, HUSCO/Ramirez Distinguished Professor of Fluid Power and Motion Control, has taught at Georgia Institute of Technology since 1974. A Fellow of ASME and IEEE, he holds degrees from M.I.T. (M.S., Ph.D.) and The University of Texas (B.S.) in Mechanical Engineering. His research focuses on system dynamics of fluid power and flexible systems, robotics, and haptic human interfaces.

Olivier Brüls
Olivier Brüls is a FNRS postdoctoral researcher in the Department of Aerospace and Mechanical Engineering (LTAS) at the University of Liège in Belgium. He received both the Ph.D. degree and the M.S. degree from the University of Liège. His research interests include flexible multibody dynamics, numerical simulation, and motion and vibration control.